



2017

Studying the Drug Delivery Kinetics of Nanosponges Using a MIP-Based Thermal Sensing Platform

Ariane Perez-Gavilan

Dublin Institute of Technology, ariane.perezgavilan@dit.ie

Christopher Pawley

Kaelin Foley

Dublin Institute of Technology

Gabrielle Tuijthof

Dublin Institute of Technology

Erik Steen Redeker

See next page for additional authors

Follow this and additional works at: <https://arrow.dit.ie/scschcpsart>

Recommended Citation

Pawley, Christopher J., et al. "Studying the Drug Delivery Kinetics of a Nanoporous Matrix Using a MIP-Based Thermal Sensing Platform." *Polymers* 9.11 (2017): 560. doi:10.3390/polym9110560

This Article is brought to you for free and open access by the School of Chemical and Pharmaceutical Sciences at ARROW@DIT. It has been accepted for inclusion in Articles by an authorized administrator of ARROW@DIT. For more information, please contact yvonne.desmond@dit.ie, arrow.admin@dit.ie, brian.widdis@dit.ie.



This work is licensed under a [Creative Commons Attribution-NonCommercial-Share Alike 3.0 License](https://creativecommons.org/licenses/by-nc-sa/3.0/)



Authors

Ariane Perez-Gavilan, Christopher Pawley, Kaelin Foley, Gabrielle Tuijthof, Erik Steen Redeker, Hanne Dillen, Kasper Eersels, Bart Van Grinsven, and Thomas J. Cleij

1 Article

2 Studying the drug delivery kinetics of nanosponges 3 using a MIP-based thermal sensing platform

4 Christopher J. Pawley ^{1*}, Ariane Perez-Gavilan ², Kaelin S. Foley ^{1,2}, Gabrielle Tuijthof ³, Erik
5 Steen Redeker ¹, Hanne Diliën ¹, Kasper Eersels ¹, Bart van Grinsven ¹ and Thomas J. Cleij ¹

6 ¹ Maastricht University, Maastricht Science Programme, P.O. Box 616, 6200 MD Maastricht, the Netherlands.

7 ² Dublin Institute of Technology, School of Chemical and Pharmaceutical Sciences, 143-149 Rathmines Road,
8 Dublin 8, Ireland.

9 ³ Zuyd University of Applied Science, Faculty of Beta Sciences and Technology, Smart devices unit, Nieuw
10 Eyckholt 300, 6419 DJ Heerlen, the Netherlands.

11 * Correspondence: c.pawley@maastrichtuniversity.nl; Tel.: +31-(0)43-388-5186

12 Academic Editor: name

13 Received: date; Accepted: date; Published: date

14 **Abstract:** The implementation of Molecularly Imprinted Polymers (MIPs) into sensing systems has
15 been demonstrated abundantly over the past decades. In this article, a novel application for a MIP-
16 based thermal sensing platform is introduced by using the sensor to characterize the drug release
17 kinetics of a nano-sized silver-organic framework. This so-called Ag-nanosponge was loaded with
18 acetylsalicylic acid (aspirin) which was used as a model drug compound in this study. The drug
19 elution properties were studied by placing the nanosponge in phosphate buffered saline solution
20 for two days and measuring the drug concentration at regular time intervals. To this extent, an
21 acrylamide-based MIP was synthesized that was able to detect aspirin in a specific and selective
22 manner. Rebinding of the template to the MIP was analyzed using a thermal sensor platform. The
23 results illustrate that addition of aspirin into the sensing chamber leads to a concentration-
24 dependent increase in the phase shift of a thermal wave that propagates through the MIP-coated
25 sensor chip. After constructing a dose-response curve, this system was used to study the drug
26 release kinetics of the nanosponge, clearly demonstrating that the metalorganic framework releases
27 the drug steadily over the course of the first hour after which the concentration reaches a plateau.
28 These findings were further confirmed by UV-VIS spectroscopy, illustrating a similar time-
29 dependent release in the same concentration range, which demonstrates that the MIP-based
30 platform can be used as a low-cost, straightforward tool to assess the efficacy of drug delivery
31 systems in a lab environment.

32 **Keywords:** Molecularly imprinted polymers, thermal detection, nanosponge, drug delivery.
33

34 1. Introduction

35 Molecular imprinting technology originally focused on the development of imprinted particles that
36 could be packed into columns for affinity separation, exploiting the affinity and selectivity to extract
37 a molecule of interest from complex matrices [1-3]. The concept was soon extended by using
38 molecularly imprinted polymers (MIPs) as antibody or enzyme mimics [4, 5]. One of the most
39 interesting applications for MIPs is their incorporation into biomimetic sensing devices as they mimic
40 the affinity of a natural receptor for its target, but are superior in terms of their chemical, thermal and
41 long term stability [6-8] and can be made through a straightforward and relatively low-cost synthesis
42 process [9]. Although MIPs have been combined with optical [10, 11], electrochemical [12-15],
43 microgravimetric [16, 17], and thermal transducers [18-22] in devices with great potential for *e.g.*
44 diagnostic applications, the translation of these lab-based devices into commercially available sensors
45 is still challenging due to difficulties with reproducibility, integrated sampling and automated signal

46 processing [23]. Therefore, this paper illustrates a new potential application for MIP-based sensing
47 systems, *i.e.* the study of the elution kinetics of drug delivery systems.

48

49 Nanosponges are virus-sized particles that can be used as smart drug delivery systems due to their
50 biodegradable polymer framework [24]. Cross-linking of the polymer leads to the formation of
51 spherical nanoparticles with a large amount of binding cavities that could be used to store drugs for
52 steady release [25]. The solubility of drugs that poorly dissolve in water can be regulated by carefully
53 tuning the composition of the polymer and balancing the ratio of lipophilic and hydrophilic segments
54 [26]. Over the past ten years, nano-sized metal-organic frameworks have emerged as an interesting
55 class of nanosponges due to their non-toxic nature and unusually large loadings of a wide variety of
56 drugs [27]. In addition, they can be made without using organic solvents and have shown to release
57 drugs in a gradual and sustaining manner which can be tuned by modifying the organic linkers
58 within their binding cavities [28]. Due to their size they can reach tightly controlled areas of the body,
59 allowing to selectively target a desired area.

60

61 Drug elution kinetics from smart drug delivery systems are traditionally studied by measuring the
62 concentration of the drug in the medium surrounding the drug carrier. The drug concentration is
63 usually determined by classic laboratory devices/techniques including radioactive assays [28],
64 fluorescent resonance energy transfer [29], liquid chromatography [30] and UV-visible spectroscopy
65 [31]. Although these methods are usually very sensitive and allow for a very accurate determination
66 of the drug concentration and hence the elution profile, most of them require expensive readout
67 devices, involve target labeling, or suffer from interference, limiting their performance in complex
68 media. Therefore selective, label-free techniques have been studied based on *e.g.* electrochemical [32]
69 and microgravimetric [33] readout methods. These platforms allow for a straightforward and
70 relatively fast analysis of the eluted medium but still require ultrasensitive, expensive readout
71 technology, conductive electrodes and involved data processing and interpretation.

72

73 Therefore, we introduce an elegant MIP-based platform for the study of drug elution from a metal-
74 organic framework in this article. Silver metalorganic frameworks were synthesized crosslinking
75 AgNO₃ with ethylenediamine in a sodium hydroxide solution leading to a sponge-like structure
76 containing a wide distribution of nanocavities. These nanosponges were loaded with the model drug,
77 acetylsalicylic acid (aspirin), one of the drugs most abundantly used for the treatment of pain, fever,
78 or inflammation that has also demonstrated to possess antithrombotic effects which positively affects
79 patients at risk for heart failure [34]. The drug elution under physiological conditions was studied in
80 the lab by applying aspirin-imprinted MIPs to aluminum electrodes and studying the propagation of
81 a thermal wave through the chip in function of an increasing concentration of acetylsalicylic acid, a
82 technique that was used successfully for the detection of dopamine in banana juice in previous work
83 [21]. Next, the constructed dose-response curve from this experiment was used to determine the
84 aspirin concentration in PBS solution containing drug eluted from the nanosponge. The results
85 demonstrated that the nanosponge releases the drugs in a burst-like manner, releasing the drug in a
86 constant fashion during the first hour, after which the concentration in the media surrounding the
87 sponge remains stable. These results were validated using UV-Visible spectroscopy, which shows a
88 similar behavior and a similar concentration range, illustrating the potential of the platform for drug
89 elution studies.

90 2. Materials and Methods

91 2.1. Chemicals

92 Acrylamide (AA), azobisisobutyronitrile (AIBN), polyvinylchloride (PVC) and silver nitrate
93 (AgNO₃) were obtained from Sigma-Aldrich. Methanol (absolute) and acetonitrile were bought at
94 Biosolve. Acetone (pure), sodium hydroxide, sulfuric acid, ethanol, salicylic acid and phosphate
95 buffered saline (PBS) tablets were acquired from VWR chemicals. Ethylenediamine (EDA), hydrazine

96 hydrate and ethylene glycol dimethacrylate (EGDM) were procured from Merck Schuchardt OHG.
97 Polydimethylsiloxane (PDMS) stamps were made with the Sylgard 184 elastomer kit from Mavom
98 NV. Aluminum chips were purchased at Brico NV and cut to the desired dimensions.

99 2.2. Synthesis of the metalorganic framework (silver nanosponge)

100 Nanosponges were synthesized by mixing aqueous AgNO₃ (5 mL, 0.4M, 2 mmol) with aqueous
101 NaOH (150 mL, 15 M, 2.25 mol). Crosslinking was initiated by the addition of aqueous EDA (1.5 mL,
102 99% w/v, 0.25 mmol) and aqueous hydrazine hydrate (0.2 mL, 80% w/v, 5.0 mmol) to the solution.
103 The mixture was then purged with N₂ and refluxed at 80 °C for 90 minutes. After cooling the reaction
104 flask to room temperature, silver nanosponges were isolated by vacuum filtration and air dried
105 before being freeze dried for 6 hours.

106 2.3. Molecular imprinting procedure

107 Pre-polymerization mixtures composed of aspirin (0.090 g, 0.5 mmol), 3 mmol AA (0.213 g) and 15
108 mmol EGDM were dissolved in 5 mL acetonitrile. Polymerization was initiated by adding 0.15 mmol
109 AIBN (0.025 g) to the pre-polymerization mixture. After sonication, the mixture was deoxygenated
110 by purging it for 5 minutes with N₂ and heated to 60 °C during 24 hours while shielding the mixture
111 from light to prevent the template from degrading. The resulting monolith was mechanically ground
112 using a Fritsch Planetary Micro Mill Pulverisette 7 premium line (700 rpm, 5 minutes, 10 mm balls)
113 and sieved using a using a Fritsch Analysette 3 for 4 hours with a 20 µm mesh. The resulting powder
114 was extracted during 96 hours at 105 °C, using a Soxhlet apparatus filled with with a mixture of
115 methanol and ethanoic acid (7:3 v/v). Finally, the MIP particles were dried for three hours in an oven
116 at 50 °C. Non-imprinted polymers (NIPs), serving as a reference, were synthesized in the same
117 manner without the presence of a template.

118 2.4. Chip preparation

119 Polished aluminium plates were cut to obtain chips with the desired dimensions (10 × 10 mm²). To
120 immobilize MIP particles onto the surface of the measurement chip, a 100 nm PVC adhesive layer
121 (0.35 wt% PVC dissolved in tetrahydrofuran) was applied onto the chip by spin coating at 3000 rpm
122 for 60 seconds with an acceleration of 1100 rpm/s. MIP and NIP particles were stamped into this
123 layer using a PDMS substrate that was covered with a monolayer of polymer particles. The PVC
124 layer was heated for 2 hours at a temperature of 100 °C way above its glass transition temperature
125 (80 °C) allowing beads to sink into the polymer layer. The samples were cooled down prior to
126 thermal measurements and any unbound particles were washed off with distilled water.

127 2.5. Selectivity test and dose-response curve

128 The thermal detection platform is described thoroughly in previous work [18-22]. Functionalized
129 chips (MIP or NIP) were pressed mechanically with their backside onto a copper block serving as a
130 heat provider. The temperature of the copper underneath the sample, T₁, was monitored by a K-type
131 thermocouple (TC Direct). This information was fed into a temperature control unit that stringently
132 controls T₁ by modifying the voltage over the power resistor (Farnell) that heats the copper, using a
133 software-based (Labview, National Instruments) proportional-integral-derivative (PID) controller
134 (P= 10, I= 8, D= 0). The functionalized side of the chip faced a polyether ether ketone (PEEK) flow cell
135 which was sealed with an O-ring to avoid leakage, defining a contact area of 28 mm² and an inner
136 volume of 110 µL. The flow cell is connected to a tubing system, allowing the administration of
137 liquids in a controlled and automated fashion by means of a syringe pump. The temperature of the
138 liquid inside the flow cell, T₂, is measured by a second thermocouple, placed 1 mm above the chip.
139 For each rebinding measurement the signal was stabilized in PBS at pH 7.4 which was used as to
140 mimic physiological conditions.

141 2.6. Loading of nanosponges with aspirin

142 Aspirin was absorbed into the nanosponges by solvent evaporation. To this extent 1.85 mmol (0.100
143 g) of the nanosponge was incubated with a 1.85 mmol aspirin in 6.2 mL of ethanol. The mixture was
144 shaken for 48 hours at 750 rpm. The solvent was removed under vacuum (30 °C, 300 mbar, 90 rpm)
145 and dried at 65 °C for 3 hours.

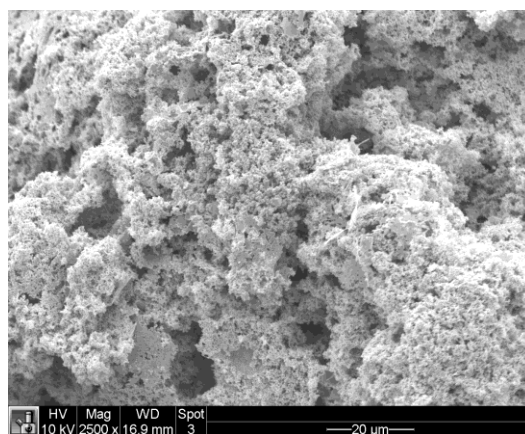
146 2.7. Drug elution analysis

147 Loaded nanosponges (0.1 g) were incubated in 300 mL PBS (pH 7.4 at 37 °C) while gently stirring at
148 100 rpm to mimic physiological conditions. Over the course of two days, 3 mL samples of the PBS
149 were taken at regular time intervals and the aspirin concentration was analyzed by both TWTA and
150 UV-visible spectroscopy to create an elution profile.

151 3. Results and Discussion

152 3.1. Surface characterization of Ag nanosponges

153 Upon synthesis the Ag nanosponges were analyzed using scanning electron microscopy (SEM). This
154 analysis reveals that the metalorganic framework indeeds has a nanosponge structure containing a
155 large set of nano-sized cavities, providing a large a surface area that can be loaded with drug
156 molecules.



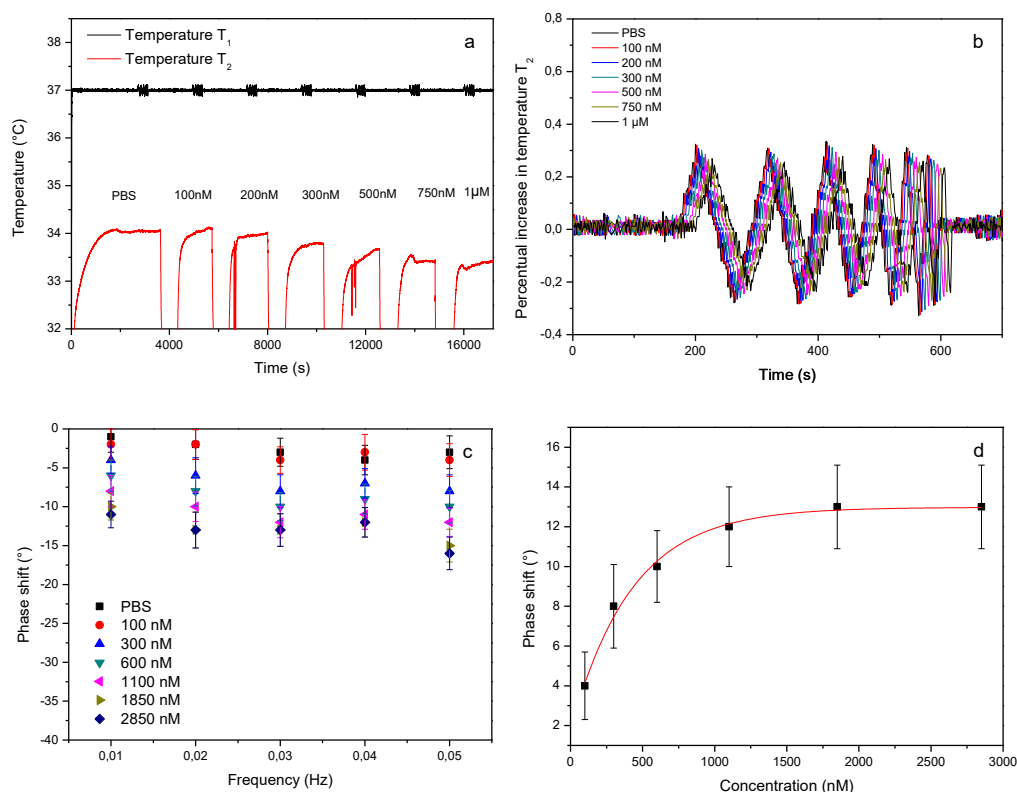
157

158 **Figure 1.** Surface analysis of an Ag-nanosponge using a scanning electron microscope at magnification 2500x.

159 3.2. Quantification of aspirin in PBS

160 To assess whether it was possible to accurately determine the concentration of drug eluted from the
161 nanosponge, a dose-response curve was constructed by exposing a MIP-coated chip to an increasing
162 concentration of aspirin in PBS. The thermal analysis clearly indicates that exposing the MIP to
163 aspirin in increasing concentrations results in a decrease of the liquid temperature inside the flow
164 chamber (Figure 2a) and a increase in the phase shift observed in the transmitted wave (Figure 2b).
165 The results in figure 2b were used to construct a thermal bode plot which shows a the phase shift for
166 each transmitted frequency in function of the cummulative concentration of aspirin present in the
167 flow cell (Figure 3c). Although the phase shift at every concentration is most pronounced at the
168 highest input frequency, the resolution appears to be optimal at 0.03 Hz. These findings are in line
169 with previously obtained results with dopamine MIPs in a similar setup [21]. The time-dependent
170 TWTA data at 0.03 Hz are used to construct a dose-response curve (figure 3d), which will be used to
171 assess the concentration of aspirin that has eluted from the Ag-nanosponge.

172



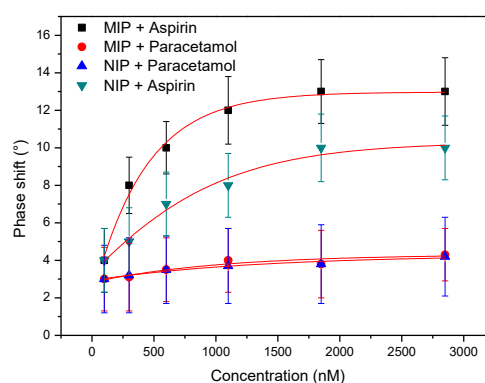
173

174

175 **Figure 2.** Aspirin rebinding analysis. The time-dependent temperature data (a) and thermal wave transport
 176 analysis spectrum (b) are shown in response to adding an increasing concentration of aspirin. The phase shift at
 177 an optimal resolution at frequency 0,03 Hz (c) and a dose-response curve (d) are constructed from these data
 178 and are plotted in function of the cummulative concentration present in the flow chamber.

179 3.3. Selectivity test

180 In order to assess whether the aspirin recognition was selective and specific, the experiment
 181 summarized in the previous section was repeated for a NIP-coated electrode. In addition, both MIP
 182 and NIP were exposed to an increasing concentration of acetaminophen (paracetamol). The resulting
 183 dose-response curves and the corresponding fits are shown in Figure 3.



184

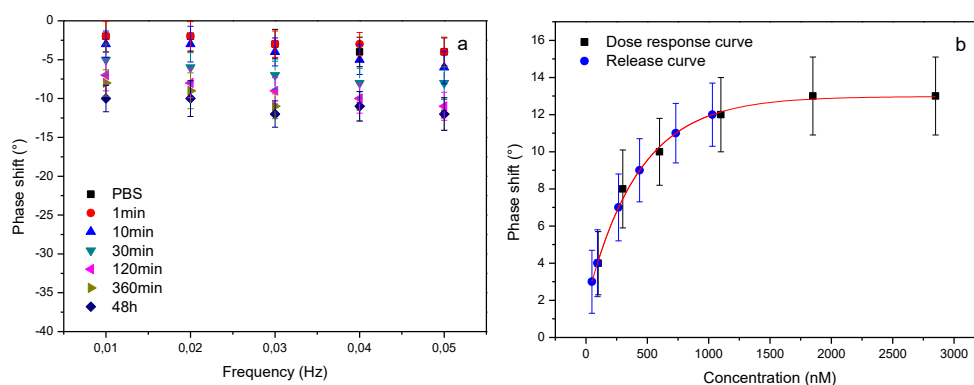
185 **Figure 3.** MIP selectivity test. The data show that exposing both the aspirin MIP and the NIP do not respond to
 186 an increasing concentration of the analogue molecule. However, the imprinting factor is limited as the difference
 187 between MIP and NIP is small.

188 The results in figure 3, illustrate that although the MIP is suprisingly selective in discriminating
 189 between paracetamol and aspirin, the imprinting factor is small. This in line with previous findings
 190 with similar AA-based MIPs and can be explained by the fact that at a neutral pH, not all binding

191 sites and functional groups on the target will be protonated (pK_a of aspirin is 3.49) [35]. The fact that
192 paracetamol only slightly increases the phase shift is surprising as the non-specific binding to the MIP
193 was expected to be similar. Although previous work has indicated that the MIP would be more
194 specific and therefore, selective at acidic pHs, the authors decided to continue measuring at a pH of
195 7.4 to simulate drug elution. The results in Figure 2 indicate that the dose-response curve is highly
196 usable and as the release pattern will be studied in PBS no interference from other molecules is to be
197 expected. However, if the concept would be extend to complex matrices in the future the MIP
198 synthesis route should be revised.

199 3.4. Thermal analysis of drug elution

200 The elution of aspirin from the nanosponges was studied by incubating them in PBS and retrieving
201 a sample from the surrounding medium after 1, 10, 30, 120 and 360 minutes and after 48 hours. The
202 elutions were diluted 5000 times with PBS to fit the linear range of the sensor. MIP-coated electrodes
203 were exposed to these diluted elutions and their response was summarized in a temperature bode
204 plot (figure 4a). The resulting phase shifts at 0.03 Hz were used to construct an elution profile that
205 was compared to the previously obtained dose response curve (figure 4b) to determine the aspirin
206 concentration in each of the eluted samples.



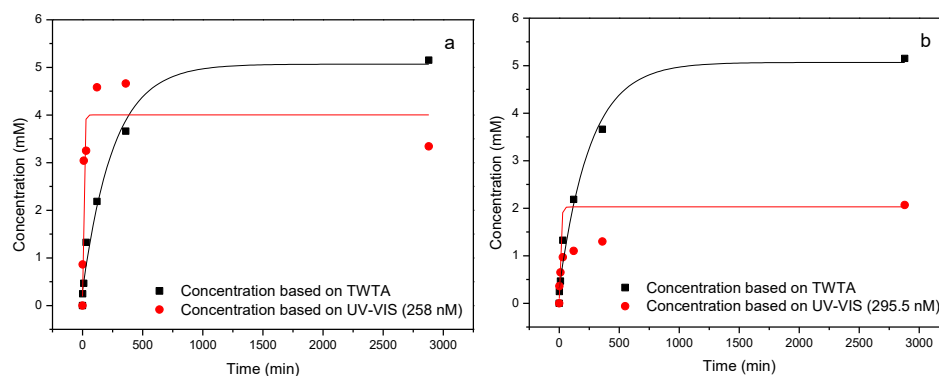
207

208 **Figure 4.** Drug elution analysis. The drug elution was studied using TWTA and the resulting Bode plot shows a
209 concentration-dependent phase shift indicating that the concentration of aspirin gradually increases with time
210 (a). The dose-response curve was used to determine the concentration in the eluted solutions (b).

211 The results obtained in Figure 4 were corrected for the dilution factor to create an elution profile that
212 validated using a gold standard reference technique, *i.e.* UV-Visible spectroscopy. The elution
213 profiles of both techniques demonstrate a similar behavior (Figure 5a): a sharp increase within the
214 first two hours after which a stable plateau is reached that does not significantly change over the next
215 two days. This indicates that the nanosponge releases the drugs in a relatively quick burst which is
216 suitable for some applications requiring immediate effect. However, to actually achieve sustained,
217 prolonged delivery of drugs the nanosponge should be functionalized with molecules that bind the
218 drug and actually release it slowly over time.

219 When analyzing the elution profile obtained by UV-Visible spectroscopy, a small decrease in the
220 concentration of aspirin can be observed over the course of two days. This can be explained by the
221 fact that some of the acetylsalicylic acid will be converted into salicylic acid in PBS. This is confirmed
222 by analyzing UV absorbance at 295.5 nm, which shows that salicylic acid is indeed present in the
223 elution and its concentration will increase slightly over the course of two days (Figure 5b). The fact
224 that this is not shown in the TWTA data is due to the fact that both compounds will bind to the MIP
225 in a similar manner [35].

226



227

228 **Figure 5.** Validation of TWTA data by UV-Visible spectroscopy. The drug elution profile derived from the TWTA
 229 data in figure 4 were compared to the drug elution profile obtained with UV-Vis and both show a initial burst
 230 of aspirin release in the first two hours in the millimolar regime (a). The decrease in aspirin concentration for the
 231 UV-vis data shown in figure 5a can be explained by conversion of aspirin into salicylic acid which is confirmed
 232 by analyzing absorbance at 295.5 nm.

233 4. Conclusions

234 The data shown in this article illustrate the potential use of a MIP-based thermal detection platform,
 235 which has previously been used for diagnostic purposes, for analyzing the drug release kinetics of
 236 drug delivery matrices. A proof-of-principle was demonstrated by validating the results obtained
 237 with the biomimetic sensor using UV-Visible spectroscopy, demonstrating a similar profile in the
 238 same concentration range. The metalorganic framework synthesized in this work appears to release
 239 the model drug, aspirin, within the first two hours. Future research should be aimed at
 240 functionalizing the framework to get to a more gradual release of the drug. In addition, loading and
 241 elution of other, potentially more relevant drugs should also be studied. As the MIP platform is
 242 generic, it can be used to study a wide variety of targets in a wide variety of matrices, by changing
 243 the MIP receptors or optimizing their selectivity or performance in more challenging media and
 244 chemical conditions (pH, temperature,...). Additionally, the platform has been recently tested for
 245 detecting molecules directly on a thermocouple wire [36], this opens up perspectives in terms of
 246 analyzing drug release *in vivo* using the proposed platform.

247 **Acknowledgments:** The authors are grateful for financial report received from the Province of Limburg
 248 (Limburg Meet project).

249 **Author Contributions:** The thermal wave transport device was designed by B.v.G. and T.J.C. TWTA
 250 measurements, data processing and interpretation were performed by B.v.G. and K.E. All nanosponges and
 251 MIPs were synthesized by C.J.P. and K.F. while input on the nanosponge synthesis and loading was provided
 252 by A.P.G. Insights on the MIP synthesis and template removal protocol was provided by E.S.R. and H.D. Input
 253 on possible experimental design were provided by G.T., C.J.P. and A.P.G. The manuscript was jointly written
 254 by P.J.W., K.E and A.P.G. All authors have given approval to the final version of the manuscript.

255 **Conflicts of Interest:** The authors declare no conflict of interest.

256 References

257

- 258 1. Mosbach, K.; Mosbach, R. Entrapment of enzymes and microorganisms in synthetic cross-linked polymers
 259 and their application in column techniques. *Acta Chem. Scand.*, **1966**, *20*, 2807-2810.
- 260 2. Sellergen, B.; Ekberg, B.; Mosbach, K. Molecular imprinting of amino acid derivatives in macroporous
 261 polymers : Demonstration of substrate- and enantio-selectivity by chromatographic resolution of racemic
 262 mixtures of amino acid derivatives. *J. Chromatogr.*, **1985**, *347*, 1-10.
- 263 3. Schirhagl, R.; Hall, E.W.; Fuereder, I.; Zare, R.N. Separation of bacteria with imprinted polymeric films.
 264 *Analyst*, **2012**, *137*, 1495-1499.

- 265 4. Vlatakis, G.; Andersson, L.I.; Müller, R.; Mosbach, K. Drug assay using antibody mimics made by molecular
266 imprinting. *Nature*, **1993**, *361*, 645-647.
- 267 5. Andersson, L.I.; Mosbach, K. Molecular imprinting of the coenzyme-substrate analogue N-pyridoxyl-L-
268 phenylalaninanilide. *Makromol. Chem., Rapid Commun.*, **1989**, *10*, 491-495.
- 269 6. Chianella, I.; Guerreiro, A.; Moczko, E.; Caygill, J.S.; Piletska, E.V.; De Vargas Sansalvador, I.M.P.;
270 Whitcombe, M.J.; Piletsky, S.A. Direct Replacement of Antibodies with Molecularly Imprinted Polymer
271 Nanoparticles in ELISA—Development of a Novel Assay for Vancomycin. *Anal. Chem.* **2013**, *85*, 8462-8468.
- 272 7. Haupt, K.; Mosbach, K. Molecularly Imprinted Polymers and Their Use in Biomimetic Sensors. *Chem. Rev.*
273 **2000**, *100*, 2495-2504.
- 274 8. Ye, L.; Haupt, K. Molecularly Imprinted Polymers as Antibody and Receptor mimics for Assays, Sensors
275 and Drug Discovery. *Anal. Bioanal. Chem.* **2004**, *378*, 1887-1897.
- 276 9. Whitcombe, M.J.; Kirsch, N.; Nicholls, I.A. Molecular Imprinting Science and Technology: A Survey of the
277 Literature for the Years 2004-2011. *J. Mol. Recogn.* **2014**, *27*, 297-401.
- 278 10. Cennamo, N.; D'Agostino, G.; Pesavento, M.; Zeni, L. High selectivity and sensitivity sensor based on MIP
279 and SPR in tapered plastic optical fibers for the detection of l-nicotine. *Sens. Actuators B Chem.* **2014**, *191*,
280 529-536.
- 281 11. Altintas, Z.; Gittens, M.; Guerreiro, A.; Thompson, K.; Walker, J.; Piletsky, S.; Tothill, I.E. Detection of
282 Waterborne Viruses Using High Affinity Molecularly Imprinted Polymers. *Anal. Chem.* **2015**, *87* (13), 6801-
283 6807.
- 284 12. Ramanaviciene, A.; Ramanavicius, A. Molecularly Imprinted Polypyrrole-Based Synthetic Receptor for
285 Direct Detection of Bovine Leukemia Virus Glycoproteins. *Biosens. Bioelectron.* **2004**, *20* (6), 1076-1082.
- 286 13. Lakshimi, D.; Bossi, A.; Whitcombe, M.J.; Chianella, I.; Fowler, S.A.; Subrahmanyam, S.; Piletska E.V.
287 Piletsky, S.A. Electrochemical Sensor for Catechol and Dopamine Based on a Catalytic Molecularly
288 Imprinted Polymer-Conducting Polymer Hybrid Recognition Element. *Anal. Chem.* **2009**, *81*, 3576-3584.
- 289 14. D., Cai; Ren, L.; Zhao, H.; Xu, C.; Zhang, L.; Ying, Y.; Wang, H.; Lan, Y.; Roberts, M.F.; Chuang, J.H.;
290 Naughton, M.J.; Ren, Z.; Chiles, T.C. A Molecular-Imprint Nanosensor for Ultrasensitive Detection of
291 Proteins. *Nat. Nanotechnol.* **2010**, *5*, 597-601.
- 292 15. Bajwa, S.Z.; Lieberzeit, P.A. Recognition principle of Cu²⁺-imprinted polymers—Assessing interactions by
293 combined spectroscopic and mass-sensitive measurements. *Sens. Actuator. B Chem.* **2015**, *207*, 976-980.
- 294 16. Ratautaite, V.; Plausinaitis, D.; Baleviciute, I.; Mikoliunaite, L.; Ramanaviciene, A.; Ramanavicius, A.
295 Characterization of Caffeine-Imprinted Polypyrrole by a Quartz Crystal Microbalance and Electrochemical
296 Impedance Spectroscopy. *Sens. Actuator. B Chem.* **2015**, *212*, 63-71.
- 297 17. Hayden, O.; Dickert, F.L. Selective Microorganism Detection with Cell Surface Imprinted Polymers. *Adv.*
298 *Mater.* **2001**, *13* (19), 1480-1483.
- 299 18. Wackers, G.; Vandenryt, T.; Cornelis, P.; Kellens, E.; Thoelen, R.; De Ceuninck; W.; Losada Pérez, P.; van
300 Grinsven, B.; Peeters, M.; Wagner, P. Array Formatting of the Heat-Transfer Method (HTM) for the
301 Detection of Small Organic Molecules by Molecularly Imprinted Polymers. *Sensors* **2014**, *14*, 11016-11030.
- 302 19. Eersels, K.; van Grinsven, B.; Khorshid, M.; Somers, V.; Püttmann, C.; Stein, C.; Barth, S.; Diliën, H.; Bos,
303 G.M.J.; Germeraad, W.T.V.; Cleij, T.J., Thoelen, R.; De Ceuninck, W.; Wagner, P. Heat-Transfer-Method-
304 Based Cell Culture Quality Assay through Cell Detection by Surface Imprinted Polymers. *Langmuir* **2015**,
305 *31* (6), 2043-2050.
- 306 20. van Grinsven, B.; Eersels, K.; Akkermans, O.; Ellermann, S.; Kordek, A.; Peeters, M.; Deschaume, O.; Bartic,
307 C.; Diliën, H.; Steen Redeker, E.; Wagner, P.; Cleij, T.J. Label-Free Detection of Escherichia Coli Based on
308 Thermal Transport Through Surface Imprinted Polymers. *ACS Sens.* **2016**, *1*, 1140-1147.
- 309 21. Peeters, M.M.; van Grinsven, B.; Foster, C.W.; Cleij, T.J.; Banks, C.E. Introducing Thermal Wave Transport
310 Analysis (TWTA): A Thermal Technique for Dopamine Detection by Screen-Printed Electrodes
311 Functionalized with Molecularly Imprinted Polymer (MIP) Particles. *Molecules* **2016**, *21*, 552.
- 312 22. Steen Redeker, E.; Eersels, K.; Akkermans, O.; Royackers, J.; Dyson, D.; Nurekeyeva, K.; Ferrando, B.;
313 Cornelis, P.; Peeters, M.; Wagner, P.; Diliën, H.; van Grinsven, B.; Cleij, T.J. Biomimetic Bacterial
314 Identification Platform Based on Thermal Wave Transport Analysis (TWTA) through Surface-Imprinted
315 Polymers. *ACS Inf. Dis.* **2017**, *3*, 388-397.
- 316 23. Selvolini, G.; Marrazza, G. MIP-Based Sensors: Promising New Tools for Cancer Biomarker Determination.
317 *Sensors* **2017**, *17*, 718.

- 318 24. Passarella, R.J.; Spratt, D.E.; Van der Ende, A.E.; Phillips, J.G.; Wu, H.M.; Sathiyakumar, V.; Zhou, L.;
319 Hallahan, D.E.; Harth, E.; Diaz, R. Targeted Nanoparticles That Deliver a Sustained, Specific Release of
320 Paclitaxel to Irradiated Tumors. *Cancer Res.* **2010**, *70*, 4550-4559.
- 321 25. Subramanian, S.; Singireddy, A.; Krishnamoorthy, K.; Rajappan, M. Nanosponges: A Novel Class of Drug
322 Delivery System – Review. *J. Pharm. Pharmaceut. Sci.* **2012**, *15*, 103-111.
- 323 26. Cavalli, R.; Trotta, F.; Tumiatti, W. Cyclodextrin-based Nanosponges for Drug Delivery. *J. Incl. Phenom.*
324 *Macrocycl. Chem.* **2007**, *56*, 209-213.
- 325 27. Horcajada, P.; Serre, C.; Vallet-Regi, M.; Sebban, M.; Taulelle, F.; Férey, G. Metal–Organic Frameworks as
326 Efficient Materials for Drug Delivery. *Angew. Chem. Int. Ed.* **2006**, *45*, 5974-5978.
- 327 28. Horcajada, P.; Chalati, T.; Serre, C.; Gillet, B.; Sebrie, C.; Baati, T.; Eubank, J.F.; Hertaux, D.; Kreuz, C.;
328 Chang, J.S.; Hwang, Y.K.; Marsaud, V.; Bories, P.N.; Cynober, L.; Gil, S.; Férey, G.; Couvreur, P.; Gref, R.
329 Porous metal–organic–framework nanoscale carriers as a potential platform for drug delivery and imaging.
330 *Nat. Mater.* **2010**, *9*, 172-178.
- 331 29. Bagalkot, V.; Zhang, L.; Levy-Nissenbaum, E.; Jon, S.; Kantoff, P.W.; Langer, R.; Farokhzad, O.C. Quantum
332 Dot-Aptamer Conjugates for Synchronous Cancer Imaging, Therapy, and Sensing of Drug Delivery Based
333 on Bi-Fluorescence Resonance Energy Transfer. *Nano Lett.* **2007**, *7*, 3065-3070.
- 334 30. Wang, Q.; Ma, D.; Higgins, P.J. Analytical method selection for drug product dissolution testing. *Dissolut.*
335 *Technol.* **2006**, *13*, 6-13.
- 336 31. Kamberi, M.; Tran, T.N. UV-visible spectroscopy as an alternative to liquid chromatography for
337 determination of everolimus in surfactant-containing dissolution media: a useful approach based on solid-
338 phase extraction. *J. Pharm. Biomed. Anal.* **2012**, *70*, 94-100.
- 339 32. Lee, R.; Jo, D.H.; Chung, S.J.; Na, H.K.; Kim, J.H.; Lee, T.G. Real-time and label-free monitoring of
340 nanoparticle cellular uptake using capacitance-based assays. *Sci. Rep.* **2016**, *6*, 33668.
- 341 33. Karlsson, J.; Atefyekta, S.; Andersson, M. Controlling drug delivery kinetics from mesoporous titania thin
342 films by pore size and surface energy. *Int. J. Nanomed.* **2015**, *10*, 4425-4436.
- 343 34. Miner, J.; Hoffhines, A. The Discovery of Aspirin's Antithrombotic Effects. *Tex. Heart Inst. J.* **2007**, *34*, 179-
344 186.
- 345 35. Meischl, F.; Schemeth, D.; Harder, M.; Köpfler, N.; Tessadri, R.; Rainer, M. Synthesis and evaluation of a
346 novel molecularly imprinted polymer for the selective isolation of acetylsalicylic acid from aqueous
347 solutions. *J. Environ. Chem.* **2016**, *4*, 4083-4090.
- 348 36. Diliën, H.; Peeters, M.; Royackers, J.; Harings, J.; Cornelis, P.; Wagner, P.; Steen Redeker, E.; Banks, C.E.;
349 Eersels, K.; van Grinsven, B.; Cleij, T.J. Label-Free Detection of Small Organic Molecules by Molecularly
350 Imprinted Polymer Functionalized Thermocouples: Toward In Vivo Applications. *ACS Sens.* **2017**, *2*, 583-
351 589.

